



HAL
open science

Elementary formulae for social distancing scenarios: Application to COVID-19 mitigation via feedback control

Michel Fliess, Cédric Join

► **To cite this version:**

Michel Fliess, Cédric Join. Elementary formulae for social distancing scenarios: Application to COVID-19 mitigation via feedback control. 2021. hal-03414354

HAL Id: hal-03414354

<https://polytechnique.hal.science/hal-03414354v1>

Preprint submitted on 4 Nov 2021

HAL is a multi-disciplinary open access archive for the deposit and dissemination of scientific research documents, whether they are published or not. The documents may come from teaching and research institutions in France or abroad, or from public or private research centers.

L'archive ouverte pluridisciplinaire **HAL**, est destinée au dépôt et à la diffusion de documents scientifiques de niveau recherche, publiés ou non, émanant des établissements d'enseignement et de recherche français ou étrangers, des laboratoires publics ou privés.

Elementary formulae for social distancing scenarios: Application to COVID-19 mitigation via feedback control

Michel Fliess^{1,3} and Cédric Join^{2,3}

Abstract

Social distancing has been enacted in order to mitigate the spread of COVID-19. Like many authors, we adopt the classic epidemic SIR model, where the infection rate is the control variable. Its differential flatness property yields elementary closed-form formulae for open-loop social distancing scenarios, where, for instance, the increase of the number of uninfected people may be taken into account. Those formulae might therefore be useful to decision makers. A feedback loop stemming from model-free control leads to a remarkable robustness with respect to severe uncertainties of various kinds. Although an identification procedure is presented, a good knowledge of the recovery rate is not necessary for our control strategy. Several convincing computer experiments are displayed.

Index Terms

Biomedical control, COVID-19, social distancing, SIR model, nonlinear feedback control, flatness-based control, model-free control, robustness, identifiability, algebraic differentiator

arXiv:2110.01712v1 [eess.SY] 4 Oct 2021

¹LIX (CNRS, UMR 7161), École polytechnique, 91128 Palaiseau, France. Michel.Fliess@polytechnique.edu

²CRAN (CNRS, UMR 7039), Université de Lorraine, BP 239, 54506 Vandœuvre-lès-Nancy, France. cedric.join@univ-lorraine.fr

³AL.I.E.N., 7 rue Maurice Barrès, 54330 Vézelize, France. {michel.fliess, cedric.join}@alien-sas.com

I. INTRODUCTION

In less than two years an abundant mathematically oriented literature has been devoted to the worldwide COVID-19 pandemic. Some of the corresponding calculations had even a significant political impact (see, *e.g.*, [1]). A novel control technique for improving the social distancing is presented here. This fundamental topic has already been tackled by many authors: see, *e.g.*, [2], [3], [6], [7], [8], [10], [12], [13], [14], [15], [21], [25], [30], [28], [36], [37], [38], [41], [43], [44], [46], [57]. Most of those papers are based on the famous *SIR* (*Susceptible-Infected-Recovered/Removed*) model, which goes back to [27] in 1927, or on slight modifications. This communication is also using the SIR model:

- When, like in several papers, the *infection rate* is the control variable, the SIR model is (*differentially flat*) ([20]). Remember that flatness-based control is one of the most popular model-based control setting, especially with respect to concrete applications: see, *e.g.*, [5], [9], [31], [32], [35], [45], [47], [49], [50], [51], [53], [54], [55], [63] for some recent publications. Note that flatness has already been utilized in [23] for studying COVID-19 but with other purposes.
- There are severe uncertainties: model mismatch, poorly known initial conditions, ... We therefore close the loop around the reference trajectory via *model-free* control, or *MFC*, in the sense of [16], [17]. MFC, which is easy to implement, has already been illustrated in a number of practical situations. Some new contributions are listed here: [22], [26], [29], [33], [39], [40], [48], [52], [58], [59], [60], [61], [64], [65]. Let us single out here the excellent work by [56] on ventilators, which are obviously related to COVID-19.

In order to be more specific consider a flat system with a single input u and a single output y . Assume that y is a flat output. Our strategy may be summarized as follows:

- 1) To any output reference trajectory y^* corresponds at once thanks to flatness an open-loop control u^* .
- 2) Let z be some measured output. Write z^* the corresponding reference trajectory. Set $u = u^* + \Delta u$, where Δu is the control of an *ultra-local* local model [16]. Its output $\Delta z = z - z^*$ is the tracking error. Closing the loop via an *intelligent controller* [16] permits to ensure local stability around z^* in spite of severe mismatches and disturbances.

Our paper is organized as follows.

- Section II shows that
 - the SIR model, where the infection rate is the control variable, is flat and the population of recovered/removed individuals is a flat output;
 - the recovery rate is identifiable in the sense of [19].
- Section III is devoted to a flatness-based control strategy, *i.e.*, to a feedforward approach. Elementary closed-form of the control and state variables are easily derived. Various scenarios, where for instance the number of uninfected persons is increased, may thus be easily suggested to decision makers.
- Closing the loop via an intelligent proportional regulator, stemming from model-free control, is the subject of Section IV. Computer simulations confirm an excellent robustness with respect to severe uncertainties.
- A time-varying recovery rate is estimated in Section V via *algebraic estimation* methods ([19]). Techniques from Section IV show however good performances if this rate is wrongly assumed to be constant.
- Some concluding remarks may be found in Section VI.

II. MODELING ISSUES

A. The SIR model

The SIR model (see, *e.g.*, [62] for a most pleasant introduction) reads:

$$\begin{cases} \dot{S} = -\beta IS \\ \dot{I} = \beta IS - \gamma I \\ \dot{R} = \gamma I \end{cases} \quad (1)$$

S , I and R , which are non-negative quantities, correspond respectively to the fractions of susceptible, infected and recovered/removed individuals in the population. We may set therefore

$$S + I + R = 1 \quad (2)$$

β , $0 < \underline{\beta} \leq \beta \leq \bar{\beta}$, which is here the control variable,¹ and the constant parameter $\gamma > 0$ are the infection and recovery rates.

B. Flatness

Equations (1)-(2) show that System (1) is flat and that R is a flat output [20]. The other system variables may be expressed as *differential rational functions* of R , *i.e.*, as rational functions of R and its derivatives up to some finite order:

$$I = \frac{\dot{R}}{\gamma} \quad (3)$$

$$S = 1 - R - \frac{\dot{R}}{\gamma} \quad (4)$$

$$\beta = -\frac{\dot{S}}{IS} = \frac{1}{S} \left(\frac{\dot{I}}{I} + \gamma \right) \quad (5)$$

Remark 1: If γ is not constant, but a differentiable function of time, Equations (3)-(4)-(5) remain valid: System (1) is still flat and R is still a flat output. Equation (5) shows however that $\dot{\gamma}$ is needed.

¹Softening social distancing implies increasing $\beta(t)$.

C. Identifiability of the recovery rate

Equation (5) yields

$$\gamma = \beta S - \frac{\dot{I}}{I}$$

γ is a differential rational function of R and β : It is thus *rationally identifiable* [19].

Remark 2: The above equation does not work for an identifiability purpose if γ is time-varying: $\dot{\gamma}$ is sitting on its right hand-side. If we assume that I and S are measured, Equation (4) yields

$$\gamma = \frac{\dot{I} - \beta IS}{I} \quad (6)$$

γ is still rationally identifiable with respect to I, S, β . It will be useful in Section V.

III. FLATNESS-BASED CONTROL

A. Preparatory calculations

Set

$$I_{\text{reference}}(t) = I_0 e^{-\lambda t}$$

where $t \geq 0, 0 \leq I_0 \leq 1$, and $\lambda \geq 0$ is some constant parameter.

Remark 3: The *reproduction number* (see, e.g., [24], [62]) is thus set to $\exp(-\lambda) < 1$. If we set $R(0) = 0$, it yields

$$R_{\text{reference}}(t) = \frac{\gamma I_0}{\lambda} (1 - e^{-\lambda t})$$

$$S_{\text{reference}}(t) = 1 - \frac{\gamma I_0}{\lambda} (1 - e^{-\lambda t}) - I_0 e^{-\lambda t}$$

and the open-loop control

$$\beta_{\text{flat}}(t) = \frac{\gamma - \lambda}{1 - \frac{\gamma I_0}{\lambda} (1 - e^{-\lambda t}) - I_0 e^{-\lambda t}}$$

Thus

$$\lim_{t \rightarrow +\infty} \beta_{\text{flat}}(t) = \frac{\lambda(\gamma - \lambda)}{\lambda - \gamma I_0} \quad (7)$$

The following inequalities are straightforward:

$$\gamma I_0 < \lambda < \gamma \quad (8)$$

$\lambda < \gamma$ follows from $\beta > 0$; $\gamma I_0 < \lambda$ follows from

$$\lim_{t \rightarrow +\infty} S(t) = 1 - \frac{\gamma I_0}{\lambda} = S(\infty) > 0 \quad (9)$$

Introduce the more or less precise quantity β_{accept} , where $\beta < \beta_{\text{accept}} < \bar{\beta}$. It stands for the ‘‘harsh’’ social distancing protocols which are ‘‘acceptable’’ in the long run. Equation (7) yields therefore

$$\frac{\lambda(\gamma - \lambda)}{\lambda - \gamma I_0} = \beta_{\text{accept}}$$

The positive root of the corresponding quadratic algebraic equation $\lambda^2 + (\beta_{\text{accept}} - \gamma)\lambda - \gamma I_0 \beta_{\text{accept}} = 0$ is

$$\lambda_{\text{accept}} = \frac{\gamma - \beta_{\text{accept}} + \sqrt{\Delta_{\text{accept}}}}{2}$$

where $\Delta_{\text{accept}} = (\gamma - \beta_{\text{accept}})^2 + 4\gamma I_0 \beta_{\text{accept}} \geq 0$. The fundamental inequality

$$\gamma I_0 < \lambda_{\text{accept}} < \gamma$$

follows from

$$\lim_{\lambda \downarrow \gamma I_0} \frac{\lambda(\gamma - \lambda)}{\lambda - \gamma I_0} = +\infty, \quad \lim_{\lambda \uparrow \gamma} \frac{\lambda(\gamma - \lambda)}{\lambda - \gamma I_0} = 0$$

Equation (9) leads to the notation

$$S_{\text{accept}}(\infty) = 1 - \frac{\gamma I_0}{\lambda_{\text{accept}}}$$

The inequality

$$S(\infty) < S_{\text{accept}}(\infty) \quad \text{if} \quad \lambda < \lambda_{\text{accept}}$$

demonstrates that the proportion of uninfected people decreases if the social distancing obligations are relaxed.

B. Two computer experiments

Set $\gamma = 0.1$, $\beta_{\text{accept}} = 0.22$. Figure 1 displays the open-loop evolutions of β , I , S when $\lambda = \lambda_{\text{accept}}$. Those behaviors are quite satisfactory.

IV. MODEL-FREE CONTROL

A. Ultra-local model

Set $\Delta I(t) = I(t) - I_{\text{reference}}(t)$, $\beta(t) = \beta_{\text{flat}}(t) + \Delta\beta(t)$. In order to take into account the various uncertainties, introduce the *ultra-local* model ([16])

$$\frac{d}{dt}\Delta I = F + \alpha\Delta\beta \quad (10)$$

- The function F , which is data-driven, subsumes the poorly known structures and disturbances.
- The parameter α , which does not need to be precisely determined, is chosen such that the three terms in Equation (10) are of the same magnitude.
- $F_{\text{est}} = -\frac{6}{\tau^3} \int_{t-\tau}^t ((t-2\sigma)\Delta I(\sigma) + \alpha\sigma(\tau-\sigma)\Delta\beta(\sigma)) d\sigma$, where $\tau > 0$ is “small”, gives a real-time estimate, which in practice is implemented via a digital filter.

B. Intelligent proportional controller

Introduce ([16]) the *intelligent proportional controller*, or *iP*,

$$\Delta\beta = -\frac{F_{\text{est}} + K_P\Delta I}{\alpha} \quad (11)$$

where K_P is a tuning gain. Equations (10) and (11) yield

$$\frac{d}{dt}\Delta I + K_P\Delta I = F - F_{\text{est}}$$

Set $K_P > 0$. Then $\lim_{t \rightarrow +\infty} \Delta I(t) \approx 0$ if the estimate F_{est} is “good,” *i.e.*, if $F - F_{\text{est}}$ is “small.” Local stability is ensured.

Remark 4: When compared to classic PIs and PIDs (see, *e.g.*, [4]), the gain tuning of the *iP* is straightforward.

C. Computer experiments

The sampling time interval is 2 hours. In Equations (10) and (11), $\alpha = 0.1$, $K_P = 1$. Figure 2 displays excellent results in spite of

- errors on initial conditions;
- the fuzzy character of any measurement of the social distancing. It is expressed by an additive corrupting white Gaussian noise $\mathcal{N}(0, 5 \cdot 10^{-3})$ on β .

V. ON THE RECOVERY RATE γ

Assume now that γ is a differentiable time function. Equation (6) yields the algebraic estimator

$$\gamma_{\text{est}} = \frac{[\dot{I}]_{\text{est}} - \beta IS}{I} \quad (12)$$

where $[\dot{I}]_{\text{est}}$ is an estimate of \dot{I} obtained along the lines developed in [34], [42] for *algebraic differentiators*. Figure 3-c displays excellent results. The flatness-based computer experiments is achieved as in Section III-B, *i.e.*, $\gamma = 0.1$ is assumed to be constant. Lack of space prevents us from displaying our convincing simulations in the more realistic situation with noise corruption.

Closing the loop via model-free control yields as demonstrated in Figures 3-a-b a rather satisfactory behavior. Should we deduce that the exact knowledge of the recovery rate is unimportant?

VI. CONCLUSION

The relevance and usefulness of such control-theoretic considerations for non-pharmaceutical mitigation policies against COVID-19 are questioned in [11]. We certainly do not claim to set aside those objections in this preliminary short study. The combination however of flatness-based and model-free controls, like in [18] for *in silico* cancer treatments, presents perhaps some major advantages:

- Flatness-based control allows to present in a straightforward way a wealth of reference trajectories in order to take into account various constraints.
- Closing the loop via model-free control permits a remarkable robustness with respect to many severe uncertainties.

Those features should of course be confirmed by further investigations.

REFERENCES

- [1] Adam D. (2020). Special report: the simulations driving the world's response to COVID-19. *Nature*, 580, 316-318.
- [2] Ames A.Z., Molnár T.G., Singletary A.W., Orosz G. (2020). Safety-critical control of active interventions for COVID-19 mitigation. *IEEE Access*, 8, 188454-188474.
- [3] Angulo M.T., Castañón F., Moreno-Morton R., Velasco-Hernández J.X., Moreno J.A. (2021). A simple criterion to design optimal non-pharmaceutical interventions for mitigating epidemic outbreaks. *J. Roy. Soc. Interface*, 18, 20200803.
- [4] Åström K.J., Murray R.M. (2008). *Feedback Systems: An Introduction for Scientists and Engineers*. Princeton University Press.
- [5] Beltran-Carbajal F., Tapia-Olvera R., Valderrabano-Gonzalez A., Yanez-Badillo H., Rosas-Caro J.C., Mayo-Maldonado J.C. (2021). Closed-loop online harmonic vibration estimation in DC electric motor systems. *Appl. Math. Model.*, 94, 460-481.
- [6] Bisiacco M., Pillonetto G. (2021). COVID-19 epidemic control using short-term lockdowns for collective gain. [arXiv:2109.00995](https://arxiv.org/abs/2109.00995)
- [7] Bliman P.-A., Duprez M. (2021). How best can finite-time social distancing reduce epidemic final size? *J. Theoret. Biol.*, 511, 110557.
- [8] Bliman P.-A., Duprez M., Privat Y., Vauchelet N. (2021). Optimal immunity control and final size minimization by social distancing for the SIR epidemic model. *J. Optim. Theory App.*, 189, 408-436.
- [9] Bonnabel S., Clayes X. (2020). The industrial control of tower cranes: An operator-in-the-loop approach. *IEEE Contr. Syst. Magaz.*, 40, 27-39.
- [10] Borri A., Palumbo P., Papa F., Possieri C. (2021). Optimal design of lock-down and reopening policies for early-stage epidemics through SIR-D models *Annual Rev. Contr.* 51, 511-524.
- [11] Casella F. (2021). Can the COVID-19 epidemic be controlled on the basis of daily test reports? *IEEE Contr. Syst. Lett.*, 5, 1079-1084.
- [12] Charpentier A., Elie R., Laurière M., Tran V.C. (2020). COVID-19 pandemic control: balancing detection policy and lockdown intervention ICU sustainability. *Math. Model. Nat. Phenom.*, 15, 57.
- [13] Di Lauro F., Kiss I.Z., Della Santina C. (2021). Optimal timing of one-shot interventions for epidemic control. *PLoS Comput. Biol.*, 17, e1008763.
- [14] Di Lauro F., Kiss I.Z., Della Santina C. (2021). Covid-19 and flattening the curve: A feedback control perspective. *IEEE Contr. Syst. Lett.*, 5, 1435-1440.
- [15] Dias S., Queiroz K., Araujo A. (2021). Controlling epidemic diseases based only on social distancing level. *J. Contr. Autom. Electr. Syst.*, <https://doi.org/10.1007/s40313-021-00745-6>
- [16] Fliess M., Join C. (2013). Model-free control. *Int. J. Contr.*, 86, 2228-2252.
- [17] Fliess M., Join C. (2021). An alternative to proportional-integral and proportional-integral-derivative regulators: Intelligent proportional-derivative regulators. *Int. J. Robust Nonlinear Contr.*, <https://doi.org/10.1002/rnc.5657>
- [18] Fliess M., Join C., Moussa K., Djouadi S.M., Alsager M.W. (2021). Toward simple in silico experiments for drugs administration in some cancer treatments. *11th IFAC Symp. Biolog. Medic. Syst.*, Ghent. <https://hal.archives-ouvertes.fr/hal-03299417/en/>
- [19] Fliess M., Join C., Sira-Ramirez H. (2008). Non-linear estimation is easy. *Int. J. Model. Identif. Contr.*, 4, 12-27.
- [20] Fliess M., Lévine J., Martin P., Rouchon P. (1995). Flatness and defect of non-linear systems: introductory theory and examples. *Int. J. Contr.*, 61, 1327-1361.
- [21] Gevertz J.L., Greene J.M., Sanchez-Tapia C.H., Sontag E.D. (2021). A novel COVID-19 epidemiological model with explicit susceptible and asymptomatic isolation compartments reveals unexpected consequences of timing social distancing. *J. Theoret. Biol.*, 510, 110539.
- [22] Gu J., Li H., Zhang H., Pan C., Luan Z. (2021). Cascaded model-free predictive control for single-phase boost power factor correction converters. *Int. J. Robust Nonlinear Contr.*, 31, 5016-5032.
- [23] Hametner C., Kozek M., Böhler L., Wasserburger A., Peng Du Z., Kölbl R., Bergmann M., Bachleitner-Hofmann T., Jakubek S. (2021). Estimation of exogenous drivers to predict COVID-19 pandemic using a method from nonlinear control theory. *Nonlin. Dyn.*, <https://doi.org/10.1007/s11071-021-06811-7>
- [24] Heesterbeek J.A.P. (2002). A brief history of R_0 and a recipe for its calculation. *Acta Biotheo.*, 50, 189-204.
- [25] Ianni A., Rossi N. (2021). SIR-PID: A proportional-integral-derivative controller for COVID-19 outbreak containment. *Physics*, 3, 459-472.
- [26] Ismail A., Noura H., Harmouch F., Harb Z. (2021). Design and control of a neonatal incubator using model-free control. *29th Medit. Conf. Contr. Automat.*, Puglia.
- [27] Kermack W.O., McKendrick A.G. (1927). A contribution to the mathematical theory of epidemics. *Proc. Royal Soc. London Ser. A*, 115, 700-721.
- [28] Köhler J., Schwenkel L., Koch A., Berberich J., Pauli P., Allgöwer F. (2021). Robust and optimal predictive control of the COVID-19 outbreak. *Annual Rev. Contr.*, 51, 525-539.
- [29] Kuruganti T., Olama M., Dong J., Xue Y., Winstead C., Nutaro J., Djouadi S., Bai L., Augenbroe G., Hill J. (2021). *Dynamic Building Load Control to Facilitate High Penetration of Solar Photovoltaic Generation*. Tech. Rep. ORNL/TM-2021/2112, Oak Ridge National Lab.
- [30] Jing M., Yew Ng K., Mac Namee B., Biglarbeigi P., Brisk R., Bond R., Finlay D., McLaughlin J. (2021). COVID-19 modelling by time-varying transmission rate associated with mobility trend of driving via Apple Maps. *J. Biomed. Informat.*, 122, 103905.
- [31] Li X., Wang Y., Guo X., Cui X., Zhang S., Li Y. (2021). An improved model-free current predictive control method for SPMSM drives. *IEEE Access*, DOI: 10.1109/ACCESS.2021.3115782
- [32] Lorenz-Meyer M.N.L., Menzel R., Dadzis K., Nikiforova A., Riemann H. (2020). Lumped parameter model for silicon crystal growth from granulate crucible. *Cryst. Res. Technol.*, 55, 2000044.
- [33] Mao J., Li H., Yang L., Zhang H., Liu L., Wang X., Tao J. (2021). Non-cascaded model-free predictive speed control of SMPMSM drive system. *IEEE Trans. Energ. Convers.*, doi: 10.1109/TEC.2021.3090427
- [34] Mboup M., Join C., Fliess M. (2009). Numerical differentiation with annihilators in noisy environment. *Numer. Algor.*, 50, 439-467.
- [35] Miuncke T. (2020). *Ein szenarienadaptiver Bewegungsalgorithmus für die Längsbewegung eines vollbeweglichen Fahrsimulators*. Springer.
- [36] Morato M.M., Bastos S.B., Cajueiro D.O., Normey-Rico J.E. (2020). An optimal predictive control strategy for COVID-19 (SARS-CoV-2) social distancing policies in Brazil. *Annual Rev. Contr.*, 50, 417-431.
- [37] Morato M.M., Pataro I.M.L., Americano da Costa M.V., Normey-Rico J.E. (2020). A parametrized nonlinear predictive control strategy for relaxing COVID-19 social distancing measures in Brazil. *ISA Trans.*, <https://doi.org/10.1016/j.isatra.2020.12.012>
- [38] Morris D.H., Rossine F.W., Plotkin J.B., Levin S.A. (2021). Optimal, near-optimal, and robust epidemic control. *Communic. Phys.*, 4, 78.
- [39] Mousavi M.S., Davari S.A., Nekoukar V., Garcia C., Rodriguez J. (2021). Model-free finite set predictive voltage control of induction motor. *12th Power Electron. Drive Syst. Techno. Conf.*, Tabriz.
- [40] Neves G., Angélico B.A. (2021). Model-free control of mechatronic systems based on algebraic estimation. *Asian J. Contr.*, <https://doi.org/10.1002/asjc.2596>
- [41] O'Sullivan D., Gahegan M., Daniel J. Exeter D.J., Adams B. (2020). Spatially explicit models for exploring COVID-19 lockdown strategies. *Trans. GIS*, 24, 967-1000.

- [42] Othmane A., Rudolph J., Mounier H. (2021). Systematic comparison of numerical differentiators and an application to model-free control. *Europ. J. Contr.*, <https://doi.org/10.1016/j.ejcon.2021.06.020>
- [43] Péni T., Csutak B., Szederkényi G., Röst G. (2020). Nonlinear model predictive control with logic constraints for COVID-19 management. *Nonlin. Dyn.*, 102, 1965-1986.
- [44] Pillonetto G., Bisiacco M., Palù G., Cobelli C. (2021). Tracking the time course of reproduction number and lockdown's effect on human behaviour during SARS-CoV-2 epidemic: nonparametric estimation. *Sci. Rep.*, 11, 9772.
- [45] Richter H., Warner H. (2021). Motion optimization for musculoskeletal dynamics: A flatness-based polynomial approach. *IEEE Trans. Automat. Contr.*, DOI: 10.1109/TAC.2020.3029318
- [46] Sadeghi M., Greene J.M., Sontag E.D. (2021). Universal features of epidemic models under social distancing guidelines. *Annual Rev. Contr.*, 51, 426-440.
- [47] Sahoo S.R., Chiddarwar S.S. (2020). Flatness-based control scheme for hardware-in-the-loop simulations of omnidirectional mobile robot. *Simul.*, 96, 169-183.
- [48] Sancak C., Yamac F., Itik, M., Alici G. (2021). Force control of electro-active polymer actuators using model-free intelligent control. *J. Intel. Mater. Syst. Struct.*, <https://doi.org/10.1177/1045389X20986992>
- [49] Sanchez J.C., Gavilan F., Vazquez R., Louembet C. (2020). A flatness-based predictive controller for six-degrees of freedom spacecraft rendezvous. *Acta Astronaut.*, 167, 391-403.
- [50] Schörghuber C., Göllés M., Reichhartinger M., Horn M. (2020). Control of biomass grate boilers using internal model control. *Contr. Eng. Pract.*, 96, 104274.
- [51] Steckler P.-B., Gauthier J.-Y., Lin-Shi X., Wallart (2021). Differential flatness-based, full-order nonlinear control of a modular multilevel converter (MMC). *IEEE Trans. Contr. Syst. Technol.*, DOI: 10.1109/TCST.2021.3067887
- [52] Sun J., Wang J., Yang P., Guo S. (2021). Model-free prescribed performance fixed-time control for wearable exoskeletons. *Appl. Math. Model.*, 90, 61-77.
- [53] Tal E.A., Karaman S. (2021). Global trajectory-tracking control for a tailsitter flying wing in agile uncoordinated flight. *AIAA Aviat. Forum.*
- [54] Thounthong P., Mungporn P., Guilbert D., Takorabet N., Pierfederic S., Nahid-Mobarekeh B., Hug Y., Bizouh N., Huangfui Y., Kumamj P. (2021). Design and control of multiphase interleaved boost converters-based on differential flatness theory for PEM fuel cell multi-stack applications. *Elect. Power Ener. Syst.*, 124, 106346.
- [55] Tognon M., Franchi A. (2021). *Theory and Applications for Control of Aerial Robots in Physical Interaction Through Tethers*. Springer.
- [56] Truong C.T., Huynh K.H., Duong V.T., Nguyen H.H., Pham L.A., Nguyen T.T. (2021). Model-free volume and pressure cycled control of automatic bag valve mask ventilator. *AIMS Bioengin.*, 8, 192-207.
- [57] Tsay C., Lejarza F., Stadtherr M.A., Baldea M. (2020). Modeling, state estimation, and optimal control for the US COVID-19 outbreak. *Scientif. Rep.*, 10, 10711.
- [58] Xu L., Chen G., Li Q. (2020). Ultra-local model-free predictive current control based on nonlinear disturbance compensation for permanent magnet synchronous motor. *IEEE Access*, 8, 127690-127699.
- [59] Xu L., Chen G., Li Q. (2021). Cascaded speed and current model of PMSM with ultra-local model-free predictive control. *Int. J. Robust Nonlinear Contr.* <https://doi.org/10.1049/elp2.12108>
- [60] Wang Y., Li H., Liu R., Yang L., Wang X. (2020). Modulated model-free predictive control with minimum switching losses for PMSM drive system. *IEEE Access*, 8, 20942-20953.
- [61] Wang Z., Wang J. (2020). Ultra-local model predictive control: A model-free approach and its application on automated vehicle trajectory tracking. *Contr. Eng. Pract.*, 101, 104482.
- [62] Weiss H. (2013). The SIR model and the foundations of public health. *Materials matemàtics*, <https://ddd.uab.cat/record/108432>
- [63] Zauner M., Mandl P., König O., Hametner C., Jakubek S. (2021). Stability analysis of a flatness-based controller driving a battery emulator with constant power load. *at-Automatisierungstech.*, 69,142-154.
- [64] Zhang Y., Jiang T., Jiao J. (2020). Model-free predictive current control of a DFIG using an ultra-local model for grid synchronization and power regulation. *IEEE Trans. Energ. Conv.*, 35, 2269-2280.
- [65] Zhang Y., Wang X., Yang H., Zhang B., Rodriguez J. (2021). Robust predictive current control of induction motors based on linear extended state observer. *Chinese J. Elec. Engin.*, 7, 94-105.

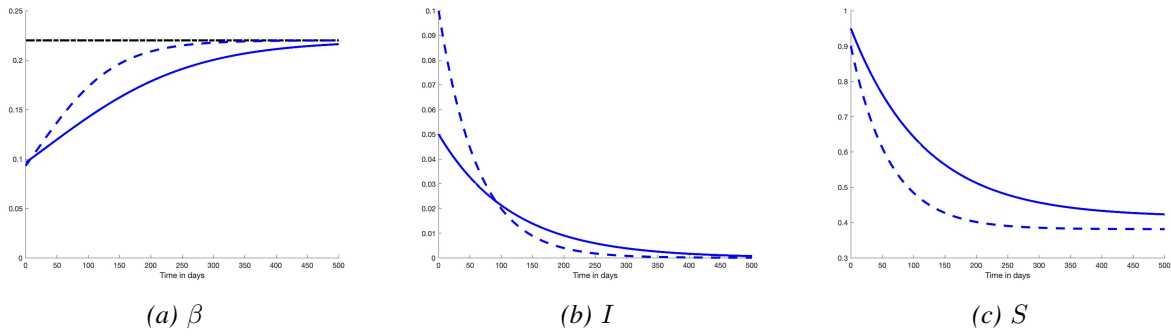


Fig. 1: Open loop: $I_0 = 0.05$ (-) and $I_0 = 0.1$ (- -)

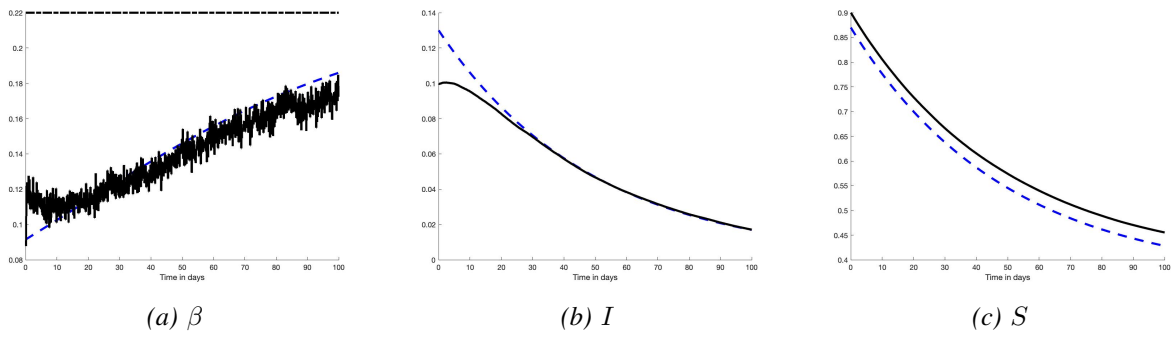
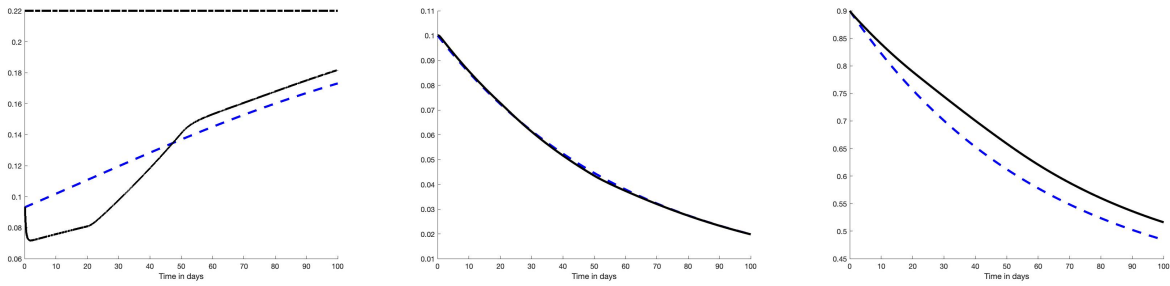
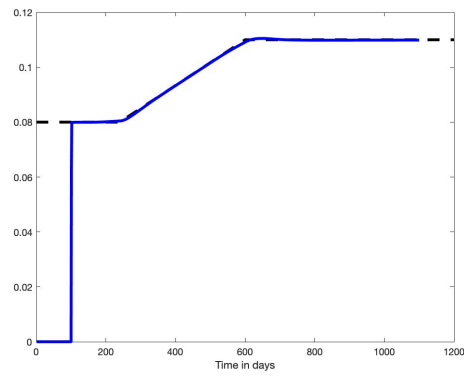


Fig. 2: Error on initial conditions and fuzzy β – blue(- -): reference trajectory



(a) β – blue(- -): reference trajectory (b) I – blue(- -): reference trajectory (c) S – blue(- -): reference trajectory



(d) γ (- -) and γ_{est} (blue -)

Fig. 3: Variable recovery rate γ